The Differential Cross Section for the Scattering of 9.48-Mev Protons by Helium

T. M. PUTNAM*
Crocker Laboratory, Department of Physics, University of California, Berkeley, California
(Received May 5, 1952)

The angular distribution of protons scattered by helium has been measured at 9.48-Mev incident proton energy in the angular range of 10° to 172.5° in the laboratory system. Ilford C-2 photographic emulsions were used for detecting the scattered particles. The geometry of the multiplate scattering chamber and the accuracy of the construction was such that the results obtained have a relative accuracy within the counting statistics and an absolute accuracy to ±3 percent. The results are given in terms of the differential cross section per unit solid angle in the center-of-mass system and are compared to the results at other energies.

I. INTRODUCTION

THE scattering of protons from helium nuclei, as with the scattering of protons from other light nuclei, is of fundamental interest in the information which the angular distribution of the scattered products can give to aid in forming a theory of nuclear forces. Proton-helium angular distribution measurements have been made in the energy range of 1 to 3.5 Mev,[1] at 5.1 Mev,[2] and at 5.8 Mev.[3] Critchfield and Dodder have set the initial pattern for the phase shift analysis of the proton-helium case with their analysis of the low energy data.[4] Further work is being carried out on the data at 5.1 and 5.8 Mev.

In addition to the angular distribution of the scattered products, information has also been obtained concerning an excited state in Li^5. Several groups have investigated the possibility of resonance scattering in the proton-helium case. The Minnesota group (reference 1) has measured the angular distribution as a function of energy and has shown the existence of a broad resonance near 2 Mev. The earlier work in this field was limited somewhat by the maximum available proton energy and the resonance was not observed.

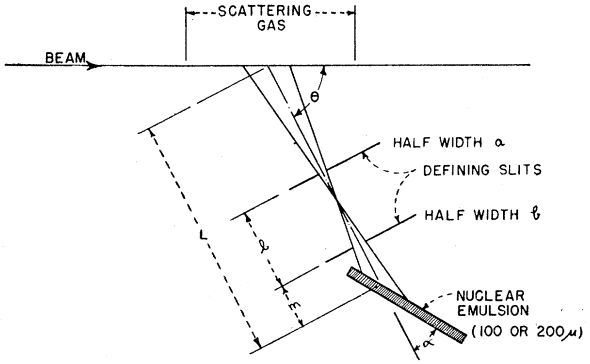

FIG. 1. Slit system geometry for scattering at angle of θ to the incident beam axis. Slit width=0.045″; plate angle=11°46′; slit separation=2.875″.

The experiment to be described is the measurement, by means of photographic emulsions, of the angular distribution of the 9.5-Mev protons scattered by a "thin" helium gas target. The 20-Mev molecular hydrogen beam from the 60-in. cyclotron in Crocker Laboratory was used as the source of protons. The molecular hydrogen breaks up into two protons on passing through the thin foil at the entrance to the scattering chamber giving a beam of protons ofapproximately 9.5-Mev energy. The scattering measurements were limited to this single energy, hence no direct evidence could be obtained regarding an excited state in Li^5. However, since photographic emulsions were used to record the scattered particles, the existence of an excited state of He^4 in the energy range of approximately 1 to 8 Mev could be established by the presence of two ranges of scattered protons. Due to the limited energy resolution in the experiment, however, no evidence was obtained concerning such an excited state in the energy range used. The work by Allred[5] on the $He^3(dp)He^4$ case has also indicated a low cross section for an excited state below 20.9 Mev.

This experiment, then, extends the energy range of the measurements of proton-helium scattering to 9.48 Mev. The angular range has also been extended to 172.5° in the laboratory. Sufficient data has been obtained to indicate that the angular distribution curve at this energy does not possess any fine structure.

II. ASSOCIATED THEORY

The angular distribution of the products of a scattering process is customarily expressed in terms of the differential cross section per unit solid angle $d\sigma(\theta)/d\omega$. The differential element of the total yield of the process may be expressed as

$$dY = Nn[d\sigma(\theta)/d\omega]d\omega,$$

where N is the number of particles in the incident beam per unit area, n is the number of target nuclei per unit area, and $d\omega$ is the solid angle subtended by the detector at the angle θ.

The geometry of the scattering system is shown in Fig. 1. The beam can be assumed to be a line source of

* Present address, Los Alamos Scientific Laboratory, University of California, Los Alamos, New Mexico.

[1] Freier, Lampi, Sleator, and Williams, Phys. Rev. **75**, 1345 (1949).

[2] C. H. Braden, Phys. Rev. **84**, 762 (1951).

[3] W. E. Kreger (to be published).

[4] C. L. Critchfield and D. C. Dodder, Phys. Rev. **76**, 602 (1949).

[5] J. C. Allred, Phys. Rev. **84**, 695 (1951).

particles since it is collimated by circular apertures to a diameter of $\frac{3}{16}$ inch, and the distance to the detector is approximately 8 inches. (It can be shown analytically[6] that the difference, between the average solid angle subtended by the detector from the extreme edges of the beam and that subtended from the axis, is completely negligible.) The number of scattering centers n may then be expressed in terms of the product $n_0 dy$, where n_0 is the number of nuclei per unit volume and dy is the element of length along the beam axis from which particles are scattered into the detector. If Y is the total number of scattered particles on the photographic plate and N is the total number of incident particles, then

$$Y = n_0 N \frac{d\sigma(\theta)}{d\omega} \int\int dy d\omega.$$

If this number is recorded in a swath along the plate of width W and length dx, it may be expressed in terms of these quantities and the slit system geometry. The result, neglecting second-order terms, is[7]

$$Y = n_0 N \frac{d\sigma(\theta)}{d\omega} \frac{4abW}{lL \sin\theta}.$$

The expression for the differential cross section per unit solid angle is then

$$d\sigma(\theta)/d\omega = (Y/W)(lL \sin\theta / n_0 N ab),$$

where a and b now represent the full slit widths. It should be noted here that the only measurements necessary in evaluating the data are the determination of the number of incident protons, the number of target nuclei, and the yield of scattered particles per unit swath width on the nuclear plate detector. The angle of the detector to the scattered particle does not enter into the determination of the cross section. This is one of the prime advantages of the geometry used in the experiment.

III. APPARATUS

The scattering chamber used in this experiment was the Nuclear Multiplate Camera of J. C. Allred *et al.*,[8] which was developed at the Los Alamos Laboratories for studying the angular distribution of the products of nuclear reactions and nuclear scattering. Figure 2 shows the general experimental arrangement. The beam from the Berkeley 60-in. cyclotron was brought out through an iron snout[9] so that the camera could be located in a field-free region. Some magnetic shielding

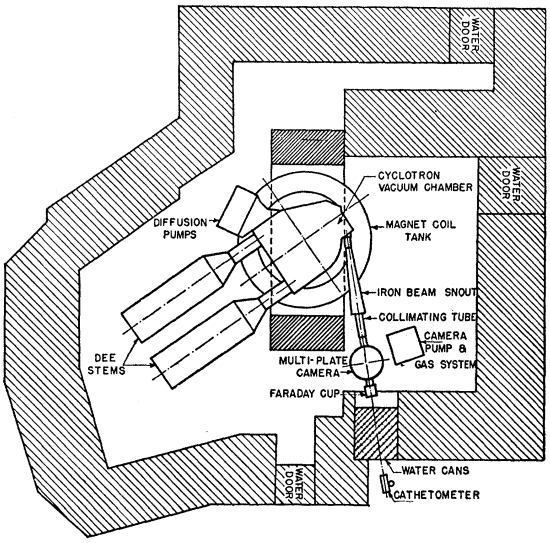

FIG. 2. Cyclotron and multiplate camera experimental arrangement.

was necessary, however, because of the proximity to the magnet yoke.

The details of the scattering chamber as well as its use in similar experiments have been given elsewhere.[8,10,11] The essential features as used in this experiment are the collimation of the beam to $\frac{3}{16}$-in. diameter, the multiple collimation of the scattered particles, eliminating an uncertainty in solid angle as discussed above, and the exposure of many plates (angles) at one time reducing the effect of variations in cyclotron output during the course of the experiment. Figure 3 shows the general collimation and plate arrangement. The nuclear emulsion plates are held in position between the outer slit ring and the wall of the scattering chamber such that the beam of scattered particles strikes the plate at a point about 3 cm from its inside edge. The arrangement allows the exact location of the plate to be determined and a repro-

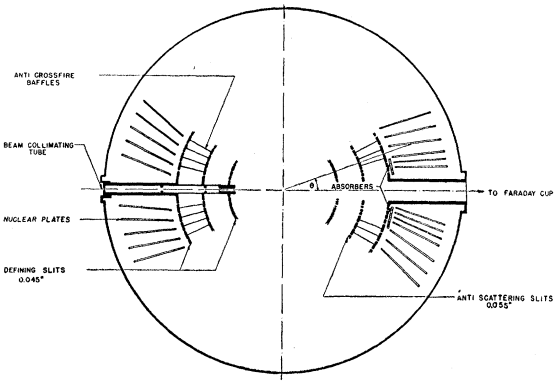

FIG. 3. Multiplate camera schematic showing beam collimation, defining slits, and nuclear plate arrangement.

[6] J. C. Allred (unpublished).
[7] The full expression for the yield with this geometry was first worked out by C. L. Critchfield at the University of Minnesota and contains terms involving the slit widths and the angle of the nuclear plate to the slit axis. However, the error introduced by neglecting these terms in less than 0.1 percent.
[8] Allred, Rosen, Tallmadge, and Williams, Rev. Sci. Instr. **22**, 191 (1951).
[9] T. M. Putnam (to be published).
[10] L. Rosen and J. C. Allred, Phys. Rev. **82**, 777 (1951).
[11] Rosen, Tallmadge, and Williams, Phys. Rev. **76**, 1283 (1949).

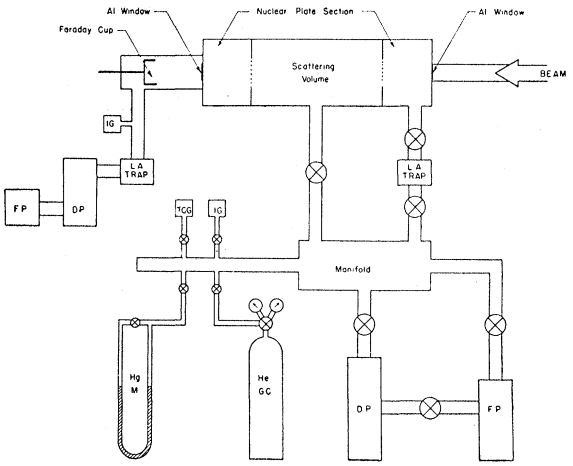

FIG. 4. Camera pump and gas system schematic. The chamber and Faraday cup pump systems are shown with the gas handling system. The symbols represent: DP, oil diffusion pump; FP, mechanical fore pump; IG, ion gauge; TCG, thermocouple gauge; HeGC, helium gas cylinder; HgM, mercury manometer; LA trap, liquid air trap.

ducible geometry is obtained. In addition, slots are provided in the outer ring assembly so that suitable foils may be inserted to slow down the scattered particles so that they will stop in the emulsion of the detector.

The angular spacing between the plates is 5° except at the forward angles. In this case three plates on one side and four on the other side of the beam axis have 2.5° spacing. With this arrangement, the angles on one side are shifted by 2.5° from the angles on the other, giving 2.5° coverage for all angles from 10° to 172.5°.

Additional features of the multiplate camera are: (1) The definining slit rings fit into recess in the camera lid and form a baffle which reduces the diffusion of water vapor from the emulsions into the scattering volume. (2) The accuracy with which the camera slit system and plate holders were machined makes it possible to obtain results which have a relative accuracy essentially within the counting statistics for each angle. The estimated error in the angle between two plates is of the order of 0.1 percent which is negligible compared to the statistical accuracy usually used (1.5–2 percent).

The camera pump and gas handling system is shown in Fig. 4. Separate oil diffusion pumps were used for the Faraday cup and the camera. It should be noted that the camera had two pump lines. The line with the liquid air trap, which was connected to the nuclear plate section, was used for evacuating the chamber and removing the condensable vapors while the second line was used for admitting the gas.

IV. NUCLEAR EMULSION TECHNIQUE

Ilford C-2 nuclear emulsion plates were used to detect the scattered particles. These were, in general, 100-micron plates, except at the forward angles where 200-micron plates were used. The principal advantages of the nuclear plate detector in a scattering experiment are (1) continuous sensitivity so that all products of the scattering process will be recorded during a run; (2) compact size enabling many angles to be measured in a single run; (3) almost complete discrimination against spurious and background particles. This is possible by the application of suitable criteria for valid tracks in the plate. The obvious disadvantages are that the data is not immediately available because of the time required for plate development and the rather extensive time required for analyzing each plate.

The analysis of the nuclear plates was made using Zeiss Jena Laboratory binocular microscopes with research microscope illuminators. Ribbon type filament lamps were used which give a uniform and intense source of light. Oil immersion objectives of 60× and compensated eyepieces of 10× were used and, with a body-tube magnification of 1.5×, a net magnification of 900× was obtained for all measurements. In order to facilitate the measurements of track lengths, a superstage driven by a precision screw was devised[12] and attached to the existing microscope stage. This superstage increased the speed and accuracy of the measurements by a factor of 3 to 5 and greatly reduced the time required to analyze a plate.

The swath width in which tracks were counted was defined by a reticule, consisting of a large ruled square subdivided into 100 sections, engraved on an optical glass disk. The disk was placed in one of the microscope eyepieces and the analyst used only that portion of the field of view within the square in selecting tracks that were to be counted.

The procedure used in analyzing a plate was as follows: From the geometry of the slit system, several initial criteria were established for all particles coming from the scattering volume: (1) Tracks must start on the surface of the emulsion. (2) They must proceed in such a direction as to have come from the scattering

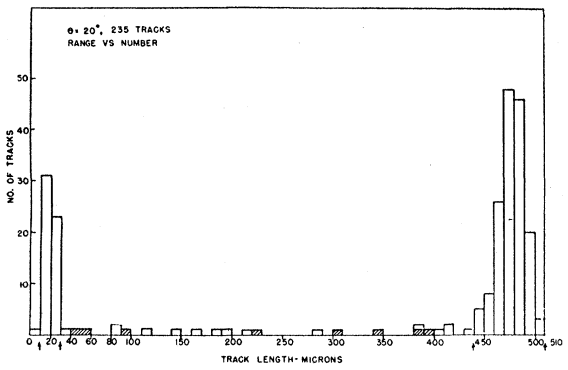

FIG. 5. Typical range *vs* number or range distribution histogram. Tracks in short peak were alpha-tracks from recoil helium nuclei. Long-range tracks were the scattered protons. Intermediate tracks were presumably slit and impurity scattered particles. Shaded areas represent tracks which fell outside the density distribution peak (see Fig. 6).

[12] T. M. Putnam and J. F. Miller (to be published).

volume. (3) They must enter the emulsion within given angular limits as determined by the slit geometry. With these criteria a preliminary measurement was made of the length of all tracks on several swaths across the plate and their position was noted in 2-mm intervals. This data when plotted as histograms gave the distribution of range and position of the tracks on the plate, as shown in Figs. 5 and 6. In Fig. 5 the short-range tracks are the recoil He nuclei which entered the plate. These tracks all fell within the density distribution. The shaded areas on the figure represent tracks which fell outside the density distribution. The other intermediate range tracks may be attributed primarily to slit-scattered particles, i.e., protons which have penetrated the slits sufficiently to lose some of their initial energy. These particles, by the nature of the defining system, have not come from the allowed scattering region or are not proceeding at the proper angle and, hence, are not counted.

From the slit geometry, it is also expected that the maximum number of tracks will occur at the intersection of the axis of the slit system with the plate and the number will fall to zero on each side of this. The position of the center of gravity of the track density histogram with respect to the edge of the plate will then enable the factor L to be determined quite accurately. In addition, from the density distribution one can be certain of including all of the tracks on the plate and, particularly at the forward angles where absorbers were used, one could determine whether or not all of the protons which pass through the slits entered the plate. This was found to be true, although the distribution was spread over a much larger portion of the plate than at larger angles where no absorbers were used.

To determine the range critierion for scattered protons, the range of the main peak of the range distribution histogram was compared with the expected proton range. This was determined from the approximate incident energy and the mechanics of the elastic scattering process, making suitable corrections for gas absorption and plate angle. By working in the opposite direction, i.e., using the measured ranges at each angle, the incident proton energy was determined. This method gave the actual value independent of any corrections for foil windows in the scattering chamber.

The track range distribution curve was also used to determine if any other process had taken place during the experiment that was observable on the plates. The limits of energy resolution are quite broad, however, because of the scattering and straggling of the tracks in the emulsion.

Thus, by applying suitable geometrical criteria together with limitations on acceptable range of valid tracks, the yield of scattered protons Y was determined. A sufficient number of complete swaths were scanned on each plate to give approximately 2500 tracks. The total swath width W was determined from the number of swaths and the known width of the reticule.

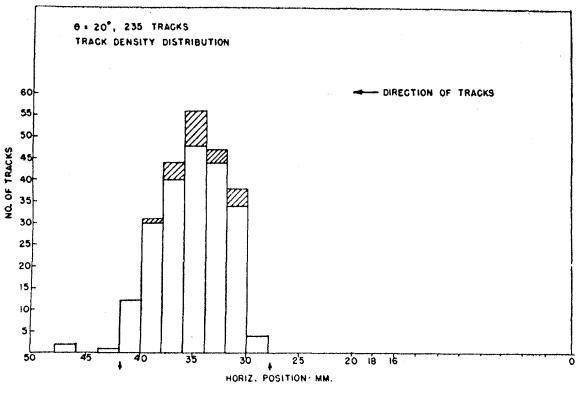

FIG. 6. Typical track density distribution histogram. Shaded areas represent tracks which fell outside the main range peaks (see Fig. 5).

V. EXPERIMENTAL PROCEDURE

The procedures used in this experiment were quite straightforward and followed the usual pattern for scattering experiments. Only a few of the more pertinent points need be mentioned. The most time-consuming part was the initial alignment of the camera. In order to fully utilize the extreme accuracy of its construction, the alignment along the beam axis was done very carefully using a cathetometer. The final data indicated that this was accomplished to better than one-quarter of one degree.

Preparation of Camera

Because of water vapor in the photographic emulsions, a rather extensive pumping time was required (four to six hours) to remove a sufficient amount of this vapor so that an appreciable error would not be introduced in the measurements. The liquid air trap in the line to the annular area containing the plates (shown in Fig. 4) was used during this period. A rate of rise of the system, with the pump and trap shut off, of 5 to 10 microns per minute was considered low enough for the experiment. The base pressure was usually in the neighborhood of 10^{-5} mm Hg at this point.

Gas Handling and Determination of n_0

The helium gas used in the experiment was taken from a tank of standard Grade A helium. No effort was made to purify the gas because of its rated purity and the almost complete discrimination against impurity-scattered particles which was possible in the counting. After the camera had been outgassed, the pump and liquid air trap were shut off from the system and the gas admitted to the desired pressure as determined by a mercury manometer.

The determination of the number of target nuclei per unit volume n_0 depended upon the accurate measure-

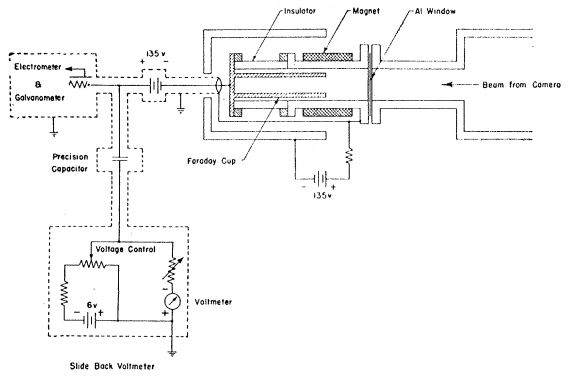

FIG. 7. Faraday cup and current integrating circuit schematic. Voltage across capacitor was maintained essentially at zero during a run by adjusting the slide-back voltmeter. Final balancing voltage was measured to determine the total charge accumulated.

ment of the pressure of the gas and its temperature. A precision cathetometer was used to measure the difference in height of the two arms of the mercury manometer. Measurements were made independently by two observers and averaged. The temperature of the gas was taken as the temperature recorded by a thermometer placed directly under the chamber. The mean of the temperature readings before and after a run was taken as the temperature of the gas during the run. Only slight differences were noted since the ambient temperature within the five-foot tanks surrounding the cyclotron remains fairly constant.

Integration of the Incident Beam and Determination of N

A separate Faraday cup unit was provided to integrate the beam passing through the chamber (Fig. 7). The cup itself was nine inches in length and $1\frac{3}{4}$ inches in inside diameter. The chamber and pump system was fastened to the scattering chamber but separated from it by a thin (0.001-inch) aluminum window. Two Alnico permanent magnets were located above and below the cup so as to create a field of the order of 1000 oersteds. The purpose of this was to trap secondary electrons produced in the cup by the positive ions. The Faraday cup was made negative with respect to ground to prevent the collection of the electrons knocked out of the window by the beam.

The primary sources of leakage which would produce errors in the value of N were assumed to be (1) ionization of the residual gas in the cup; (2) secondary electrons escaping from the cup; (3) conduction along the insulator surfaces.

Since the pressure in the Faraday cup was maintained in the range of 10^{-7} mm Hg, ionization of the residual gas should be a negligible factor and conduction along the inner surface of the insulator would be essentially eliminated. To check for the possibility of secondary electrons escaping from the cup, the cup was made positive with respect to the case. A positive charge placed on the integration condenser was neutralized indicating negative integration. No integration was observed with zero potential on the cup. In the first case, secondary electrons from the surrounding surfaces were possibly the cause, but it is more likely that it was due to leakage through the air as discussed below. The fact that no integration was observed when the cup was at zero potential indicates the effectiveness of the magnetic field in stopping secondary electrons from leaving the cup. In addition, the length of the cup and the large diameter gave added assurance that secondary electrons would not escape.

The only leakage point that needed correcting was the apparent conduction through the air and along the outside of the Faraday cup insulator. Since the experiment was performed inside the cyclotron water barrier, the radiation field (neutron and gamma ray) present when the beam was on was quite high. This apparently produced sufficient ionization of the air to cause conduction along the outside of the cup insulator. This leakage was essentially eliminated by the use of an electrostatic shield placed over the cup and put at a potential negative with respect to ground and of approximately the same value as that of the cup. This placed the cup and insulator essentially in a field-free region eliminating the leakage across the insulator. Checks of the over-all circuit indicated a total leakage current of the order of 3×10^{-12} ampere. Hence, no corrections were made to N (the number of incident protons) for leakage in the integrating circuit.

Figure 7 also shows the general circuit used for integrating the current. An accurately calibrated precision capacitor of 1.075-microfarad capacity was used to integrate the charge. The electrometer and galvanometer circuit was used to indicate the voltage on the capacitor. The voltage was maintained essentially at zero during a run by means of an associated slide-back voltmeter circuit. At the end of a run the voltage on the slide-back voltmeter, which was required to completely neutralize the accumulated charge on the condenser was measured with a Leeds and Northrup type K potentiometer and a General Radio type 654A decade voltage divider. A small drift in the electrometer was always present even with the capacitor discharged. A correction for this was applied by noting the zero drift at the end of each run.

The integrating capacitor was calibrated by means of comparison with a standard capacitor made commercially by the General Radio Company. This secondary standard was checked against the capacity of a Bureau of Standards calibrated condenser. The comparison was made with a General Radio capacitance bridge by two different observers. The value given was 1.075 ± 0.005 microfarads.

Exposure of the Plates

The exposure to be used for each run was determined from the results of a preliminary run. Examination of

the density of the tracks on the plates from this run indicated the general exposure needed for various angles to take account of the large variation in scattering cross section with angle. The exposures for the various runs are given in Table I.

A background run was also made to determine the presence of protons scattered from water vapor and other impurity gases other than those known to be present in the helium. This run was made following the same procedure as that used in handling the system for a regular exposure with the exception that no helium gas was admitted. The results of this run indicated that corrections were necessary only at the forward angles.

VI. CORRECTIONS

The techniques used in obtaining the data from the nuclear plates have already been discussed. Certain corrections were made to the raw data to correct for the effect of the absorbers used at the forward angles, for inherent background and for scattering from impurities in the gas.

The correction for absorbers at the forward angles was made for the loss of particles in a given swath width due to multiple scattering in the absorber. The amount of the correction was determined from data supplied by the Microscopy Laboratory at Los Alamos, which was obtained using the graphical method devised by Dickinson and Dodder.[13] This correction amounted to approximately six percent for the 0.008-inch aluminum absorbers used.

Background corrections were necessary due to the water vapor given off from the plates. These corrections were determined from an analysis of plates exposed in the background run. The number of tracks per centimeter swath width which would have been included in the normal counting at each angle was determined from the range analysis of the background plate at the same angle. This number was normalized for the rate of rise taken prior to each run as compared to that of the background run and for the integrated current used. The correction amounted to less than one percent at 10 degrees and above 20 degress was small enough (<0.03 percent) to be neglected.

The correction for impurity scattering due mainly to nitrogen in the helium gas was based on pure Coulomb scattering. By calculating the expected mean proton ranges of particles scattered from nitrogen and oxygen and comparing this with the accepted range for counting tracks on each plate, the angles over which a correction had to be applied were determined. It was found that below 37.5 degrees, particles scattered from nitrogen or oxygen would not be resolved from the main proton peak.

In order to determine the amounts of impurities in the helium gas used, an analysis was made of the gas by Dr. Amos Newton of the Radiation Laboratory using a Consolidated 180° Focusing Mass Spectrograph. The results of this analysis showed the primary contaminants to be hydrogen—0.02 percent, nitrogen—0.02 percent, and oxygen—0.01 percent. Using these figures and the cross sections for the Coulomb scattering of protons from nitrogen and oxygen, corrections were determined for impurity scattering. These amounted to approximately 0.5 percent at 10 degrees and were completely negligible at 20 degrees. No corrections were necessary for the hydrogen present due first to the smaller proton-proton scattering cross section in this energy range[14] and, secondly, to the fact that the ranges would be resolved above 15 degrees.

The alignment of the camera with the beam axis was determined from a graphical analysis of the data taken from the two sides of the beam. The above corrections were applied to the raw data and the results were compared. This analysis indicated that the beam was not exactly coaxial with the camera. A shift of laboratory angles of 0.2 degree was indicated and the final results were corrected for this shift.

Above 20 degrees there were no other corrections made to the data. One other source of background is open to question, however, This enters in the low energy "tail" of the range distribution peak. The incident proton beam was not monoenergetic and had a low energy tail from the nature of its production. This would similarly introduce a low energy tail on the range distribution. On the other hand, protons scattered by the slits would lose some energy and would contribute to this effect. In making the selection of the lower energy limit for acceptable tracks on the plate, this had to be considered. From an examination of the range distribution curves for each plate, it appears that the selection of ranges used would take care of this effect. Further corrections, if any, would be less than one percent and open to considerable error.

The effect of multiple scattering in the gas was also investigated. The loss of particles due to this effect was found to be completely negligible. The largest effect would have been at the backward angles where the scattered particle energy is of the order of 3 Mev. Calculations (based on reference 13) indicated that less than one percent of the particles would be deviated by only a few thousandths of a degree and, hence, the effect was completely negligible.

TABLE I. Experimental data for various runs.

Run	Gas pressure (cm Hg)	Gas temperature (°C)	Integrated current (micro-coulombs)
1	20.031	25.15	9.402
2	5.162	25.80	4.412
4	20.400	28.20	10.183
5	37.280	26.80	27.374
6	10.370	26.20	5.552

[13] W. C. Dickinson and D. C. Dodder, Los Alamos Report No. 1182 (1950).

[14] R. R. Wilson, Phys. Rev. **71**, 384 (1947).

TABLE II. Measured cross sections as a function of angle in the center-of-mass system at 9.48-Mev incident particle energy. (Laboratory angles shifted 0.2 degree.)

θ	Ω	$[d\sigma(\Omega)/d\omega] \times 10^{24}$				
		1	2	4	5	6
9.8	12.2		1.1415			
10.2	12.8		0.9947			
12.3	15.3		0.6596			
12.7	15.9		0.6294			
14.8	18.4		0.5336			
15.2	19.0		0.5086			
17.3	21.5		0.4754			0.4662
20.2	25.2		0.4126			0.4018
22.3	27.7					0.3780
25.2	31.3					0.3580
27.3	33.9					0.3382
30.2	37.4			0.3116		0.3076
32.3	40.0			0.3016		0.3099
35.2	43.5			0.2804		
40.2	49.5			0.2392		
42.3	52.0			0.2322		
50.2	61.3			0.1719		
52.3	63.7			0.1668		
60.2	72.7	0.1195				
67.3	80.6				0.0822	
70.2	83.8				0.0715	
72.3	86.1				0.0653	
80.2	94.5				0.0431	
85.2	99.6				0.0322	
90.2	104.7				0.0278	
92.3	106.8				0.0251	
97.3	111.7				0.02302	
100.2	114.4				0.0220	
102.3	116.4				0.02302	
110.2	123.8				0.0273	
115.2	128.3				0.0333	
120.2	132.7				0.0392	
122.3	134.5				0.0423	
130.2	141.2				0.0527	
135.2	145.4				0.0562	
140.2	149.4				0.0669	
142.3	151.1			0.0686		
150.2	157.3			0.0802		
152.3	159.0			0.0809		
160.2	165.0			0.0854		
162.3	166.7			0.0867		
170.2	172.6			0.0922		
172.3	174.2			0.0967		

VII. RESULTS

The corrected results of the measurements of the angular distribution for the scattered protons are given in Table II and plotted in Fig. 8 in terms of the differential cross section per unit solid angle in the center-of-mass system. The data obtained from the two sides of the beam are distinguished by the solid circles and triangles. For the data at each angle approximately 2500 tracks were counted, giving a standard deviation of ± 2 percent. For the point at 60.2° in the laboratory system, however, only 547 tracks were obtained, giving ± 4.3 percent statistical accuracy. The plate peeled so badly before analysis could be completed that further counting would have been quite inaccurate; therefore the preliminary count was used.

In general, the internal consistency of the data for each run indicates an accuracy within the counting statistics. At the check points between runs, the differences are less than three percent which gives an indication of the reproducibility of the experimental conditions from run to run, as well as giving some confidence in the absolute accuracy of the data.

The factors whose errors enter into the over-all accuracy of the data are the current integration, measurement of the gas pressure and temperature, personnel factors in reading the plates, the calibration of the eyepiece reticule in the microscope, and the measurement of geometrical factors of the multiplate camera.

The accuracy of the current integration depended primarily on the calibration of the integrating condenser. The capacity of the standard capacitor used was given to ± 0.1 percent. From the spread of values obtained in making the calibration, the integrating capacity was given to ± 0.5 percent. A precision voltmeter was used to measure the voltage and the zero drift of the electrometer circuit during integration was included. As discussed earlier, numerous checks were made on the leakage of the Faraday cup and current integration system. One check was open to question, however. This is the leakage due to the ionization of the air around the cup. Checks were made prior to operation with a one-gram radium beryllium neutron source and with the radiation from the internal beam of the cyclotron. No check was made with the beam passing through the scattering chamber but blocked off from the Faraday cup. Since the electrostatic shield around the cup completely stopped any leakage in the tests that were made, it was felt at the time that this source of error had been eliminated and that no further tests were necessary. A probable error of ± 1 percent, however, appears to be a valid figure.

From the reproducibility of the measurements of the gas pressure and the necessary application of a correction for expansion of the mercury in the manometer, the probable error to be assigned to the gas pressure measurement is ± 0.2 percent. The temperature of the gas was measurable to ± 0.1 degree out of 25 to 30 degrees, giving a probable error of ± 0.5 percent.

The probable error in measurement of Y, the yield on each plate is somewhat difficult to assign. Frequent checks of the count on a single swath by two observers indicated, however, an over-all accuracy of better than one percent. Since these checks were made under possibly very favorable conditions, a more conservative figure for the probable error due to personnel factors would be ± 1.5 percent. For the calibration of the reticule from the spread in values obtained, a probable error ± 0.4 percent can be assigned.

The measurements of geometrical factors for the nuclear plate camera have an estimated probable error of less than one percent. These are: a, b -0.5 percent; -0.1 percent; L as measured on the plate -0.1 percent.

The resulting root-mean-square probable error for the measurements which enter into the cross section calculations is 2.1 percent. Considering the average statistical accuracy of 2 percent, a figure of ± 2.9 percent

for the absolute standard error can be assigned to all points in the angular range of 25 to 175 degrees (CM). The point at 72.7 degrees (CM), because of its statistical accuracy of 4.3 percent, can be assigned a probable error of ± 4.75 percent. At the more forward angles where large corrections are needed for the absorbers, an absolute standard error ± 5.0 percent can be assigned.

Figure 9 shows how the angular distribution of the scattered protons varies with the incident energy. It is interesting to note the similarity in shape of the distribution curves at 3.58, 5.8, and 9.48 Mev. The data at 5.1 Mev also agrees fairly well with that at 5.8 Mev except for the point near 150 degrees. This point is open to question because of the disagreement in shape with that of the other curves. The sudden change in shape of the distribution curve in the neighborhood of the resonance near 2 Mev (see reference 1) is also quite evident. Also included in the same figure is the differential cross section curve for pure Coulomb scattering as calculated for 9.48 Mev.

VIII. DETERMINATION OF BEAM ENERGY

As indicated previously the beam energy can be determined directly from the scattered particle energy in this experiment, eliminating corrections for intervening windows. The method, of course, gives the average value of the energy during a given run.

For the determination of the beam energy, the mean value of the proton range at each angle was obtained

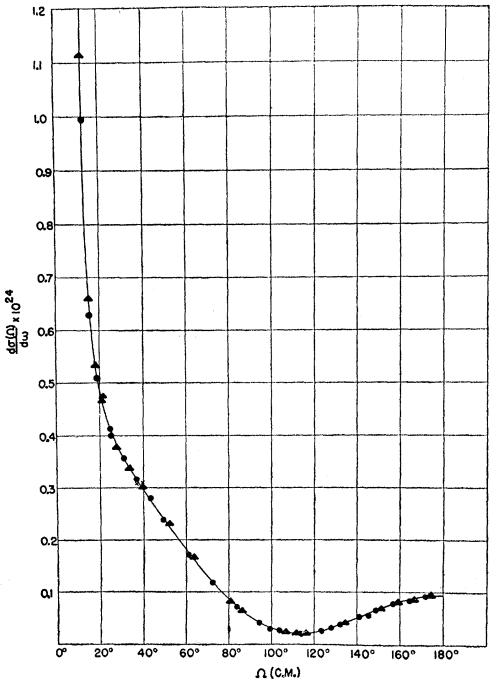

FIG. 8. The differential cross section as a function of angle in the center-of-mass system for the scattering of 9.48-Mev incident protons from helium. Points obtained from the two sides of the beam axis are indicated by closed circles and triangles.

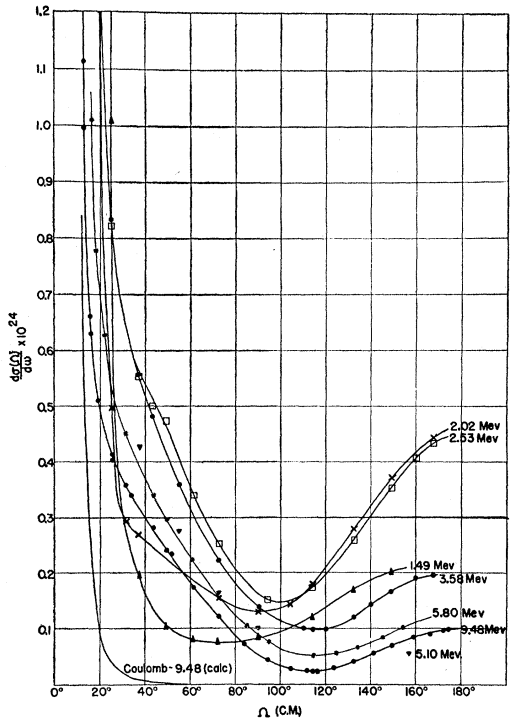

FIG. 9. Proton-helium scattering cross sections per unit solid angle in the center-of-mass system for various incident proton energies. For 5.1 Mev only the experimental points are shown.

from the range distribution analysis. This gave the mean-projected-range on the surface of the emulsion. Corrections were made for plate angle and emulsion shrinkage in determining the absolute mean range of the protons in the emulsion and allowances were made for the energy loss in the gas between the scattering center and the plate. The energy loss in the gas was determined by calculating the emulsion equivalent of the gas and assuming that the emulsion equivalent of one centimeter of air is equivalent to five microns of emulsion at N.T.P. The emulsion equivalent of the gas for each run was calculated from the relation

$$\frac{P_{\text{targ}}}{76}\times\frac{288}{T_{\text{targ}}}\times 5LS=\text{emulsion equivalent in microns},$$

where L=path length in the gas as determined from the center of gravity of the track density distribution on the plate. S is the stopping power of the gas with respect to that of air. This was determined over the energy interval in question from the range energy curves for protons in air and helium given by Aron, Hoffman, and Williams.[15] The value used was 0.155 for the stopping power of helium relative to air for the energy range of 3 to 9 Mev. The resulting values for the energy at each angle were averaged giving for the mean

[15] Aron, Hoffman, and Williams, unpublished University of California Radiation Laboratory Report No. 121 (Revised) (1949).

value of the energy from all the 47 plates 9.48±0.15 Mev.

ACKNOWLEDGMENTS

It is a pleasure to acknowledge the encouragement and guidance of Professors E. M. McMillan, A. C. Helmholz, and J. G. Hamilton during the course of this work. Sincere thanks are also due Dr. Louis Rosen, for making this experiment possible by the use of the multiplate camera; Dr. J. C. Allred and Dr. R. O. Bondelid for their assistance in making the runs; Dr. Alice H. Armstrong for many helpful discussions.

The reading of the photographic plates was done in part at the Microscopy Laboratory at Los Alamos, chiefly by Mrs. J. Gammel and Mrs. M. Downs. Mrs. R. Gibbs and Mrs. T. M. Putnam assisted in the final counting of the tracks.

Thanks are also due the members of the Crocker Laboratory staff who contributed in many ways towards the completion of this work.

PHYSICAL REVIEW VOLUME 87, NUMBER 6 SEPTEMBER 15, 1952

Interaction between Electron and One-Dimensional Electromagnetic Field

NATHAN ROSEN
Department of Physics, University of North Carolina, Chapel Hill, North Carolina
(Received May 14, 1952)

For a single electron interacting with the quantized transverse electromagnetic field it is found that, in the one-dimensional case, the Schrödinger equation can be put into a form like that of a system of coupled harmonic oscillators. From the classical frequencies of the normal modes of oscillation of such a system the quantal energy can be determined. While the perturbation method gives a logarithmic divergence in the interaction energy, one finds by the present method that the energy diverges like the square root of a logarithm.

A QUESTION which does not appear to have received a satisfactory answer is whether the divergences arising in the interaction between a point electron and the quantized electromagnetic field are inherent in the problem or are due to the methods of calculation employed. The purpose of this paper is to attempt to throw some light on this question by considering a simplified case in which the electron and the field are constrained to one-dimensional motion. This may be regarded as a continuation of earlier work on one-dimensional fields.[1]

Let us consider first the more general case of a single electron, described by the Dirac equation, interacting with a quantized electromagnetic radiation field. Thus we do not make use of the hole theory of the vacuum. Nor do we concern ourselves here with the interaction with the longitudinal part of the field; this will be regarded as already included in the mass term of the Dirac equation. If we think of the system as satisfying a periodicity condition in a fundamental cube of side L, we can expand the field in a set of monochromatic plane polarized waves of proper frequencies with quantized amplitudes.[2] Let us label these modes of oscillation of the field by an integer λ. The Hamiltonian for the system can then be written

$$H=c\boldsymbol{\alpha}\cdot\mathbf{p}+mc^2\beta-e\boldsymbol{\alpha}\cdot\textstyle\sum_\lambda \mathbf{A}_\lambda+H_0, \tag{1}$$

where $\mathbf{p}$ is the electron momentum, H_0 is the Hamiltonian of the field,

$$H_0=\tfrac{1}{2}\textstyle\sum_\lambda(P_\lambda^2+\omega_\lambda^2Q_\lambda^2-\hbar\omega_\lambda), \tag{2}$$

and

$$\mathbf{A}_\lambda=c\pi^{\frac{1}{2}}L^{-\frac{3}{2}}\boldsymbol{\varepsilon}_\lambda[Q_\lambda(e^{i\mathbf{k}_\lambda\cdot\mathbf{r}}+e^{-i\mathbf{k}_\lambda\cdot\mathbf{r}}) +(i/\omega_\lambda)P_\lambda(e^{i\mathbf{k}_\lambda\cdot\mathbf{r}}-e^{-i\mathbf{k}_\lambda\cdot\mathbf{r}})] \tag{3}$$

is the vector potential for the degree of freedom labeled by λ at the position of the electron specified by the vector $\mathbf{r}$. Here $\mathbf{k}_\lambda$ is $2\pi/L$ times a vector with integer components (positive and negative) depending on λ, $\omega_\lambda=c|\mathbf{k}_\lambda|$, and $\boldsymbol{\varepsilon}_\lambda$ is the polarization vector, orthogonal to $\mathbf{k}_\lambda$. The amplitudes Q_λ and P_λ are pairs of conjugate variables satisfying the usual commutation relations for coordinates and momenta. In H_0 the zero-point energy has been subtracted.

We now consider the Schrödinger equation for a stationary state of energy E,

$$H\psi=E\psi, \tag{4}$$

where the operator H is given by (1) with $\mathbf{p}=-i\hbar\nabla$, $P_\lambda=-i\hbar(\partial/\partial Q_\lambda)$.

To solve this equation let us write the wave function ψ as an expansion of the form

$$\psi=\textstyle\sum_{(n)} a_{n_1n_2\cdots n_\lambda\cdots}U_{n_1n_2\cdots n_\lambda\cdots} \times\exp[i(\mathbf{p}'/\hbar-n_1\mathbf{k}_1-n_2\mathbf{k}_2\cdots)\cdot\mathbf{r}]. \tag{5}$$

Here

$$U_{n_1n_2\cdots n_\lambda\cdots}=u_{n_1}(Q_1)u_{n_2}(Q_2)\cdots u_{n_\lambda}(Q_\lambda)\cdots, \tag{6}$$

[1] N. Rosen, Phys. Rev. **71**, 833 (1947), and **76**, 202 (1949); W. Sollfrey and G. Goertzel, Phys. Rev. **83**, 1038 (1951).

[2] See, e.g., W. Heitler, *The Quantum Theory of Radiation* (Oxford University Press, London, 1944), second edition.